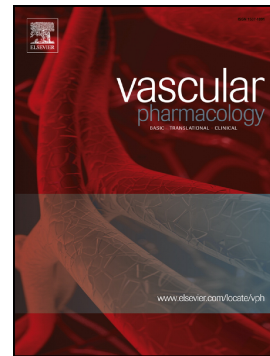


## Accepted Manuscript

Ex vivo microangioCT: Advances in microvascular imaging

Ruslan Hlushchuk, David Haberthür, Valentin Djonov



PII: S1537-1891(18)30230-1  
DOI: doi:[10.1016/j.vph.2018.09.003](https://doi.org/10.1016/j.vph.2018.09.003)  
Reference: VPH 6520  
To appear in: *Vascular Pharmacology*  
Received date: 18 June 2018  
Revised date: 6 September 2018  
Accepted date: 20 September 2018

Please cite this article as: Ruslan Hlushchuk, David Haberthür, Valentin Djonov , Ex vivo microangioCT: Advances in microvascular imaging. *Vph* (2018), doi:[10.1016/j.vph.2018.09.003](https://doi.org/10.1016/j.vph.2018.09.003)

This is a PDF file of an unedited manuscript that has been accepted for publication. As a service to our customers we are providing this early version of the manuscript. The manuscript will undergo copyediting, typesetting, and review of the resulting proof before it is published in its final form. Please note that during the production process errors may be discovered which could affect the content, and all legal disclaimers that apply to the journal pertain.

***Ex Vivo MicroangioCT: Advances in Microvascular Imaging******Ruslan Hlushchuk\*, David Haberthür and Valentin Djonov****Institute of Anatomy, University of Bern, Bern, Switzerland**\* Correspondence to:**PD MD Ruslan Hlushchuk**Institute of Anatomy**University of Bern**Baltzerstrasse 2**CH-3012 Bern, Switzerland**Email: ruslan.hlushchuk@ana.unibe.ch***Abstract**

Therapeutic modulation of angiogenesis is believed to be a prospective powerful treatment strategy to modulate the microcirculation and therefore help millions of patients with cardiovascular and cancer diseases. The often-frustrating results from late-stage clinical studies indicate an urgent need for improved assessment of the pro- and anti-angiogenic compounds in preclinical stage of investigation. For such a proper assessment, detailed vascular visualization and adequate quantification are essential. Nowadays, there are few imaging modalities available, but none of them provides non-destructive 3D-visualization of the vasculature down to the capillary level. In many instances, the approaches cannot be combined with the subsequent histological or ultrastructural analysis.

In this review, we address the latest developments in the microvascular imaging, namely, the microangioCT approach with a polymer-based contrast agent ( $\mu$ Angiofil). This approach allows time-efficient non-destructive 3D-imaging of the organ and its vasculature including the finest capillaries. Besides the superior visualization, the obtained detailed 3D information on the organ vasculature enables its 3D-skeletonization and further quantitative analysis.

Probably the only significant limitation of the described approach is that it can be used only *ex vivo*, i.e., no longitudinal studies.

In spite of this drawback, microangioCT with  $\mu$ Angiofil is a relatively simple and straightforward tool with a broad application range for studying physiological and pathological alterations in the microvasculature of any organ. It provides microvascular imaging at unprecedented level and enables correlative microscopy.

## **Vascular visualization in the angiogenic research**

Angiogenesis, the de novo formation of new blood vessels, is a heavily investigated biological process with enormous medical, scientific and economic impact [1]. Therapeutic angiogenesis is believed to be a powerful prospective treatment strategy to modulate the microcirculation and therefore help millions of cardiovascular and cancer patients. This results in more than 4000 clinical trials dealing with angiogenesis (<http://clinicaltrials.gov>). Worldwide, the vascular biology field focuses on identification of potent angiomodulating substances with potential future clinical application. The analysis of preclinical testing demonstrated that only around 0.1% of all tested compounds are passing to the clinical trials in human patients [2]. Unfortunately, the often-frustrating results from late-stage clinical studies indicate an urgent need for improved assessment of the pro- and anti-angiogenic compounds in preclinical models [3, 4].

The detailed vascular visualization and adequate quantification are essential not only for proper assessment of novel angiomodulating therapies but also for many other vasculature-related/involving processes or diseases. In this review we focus on the latest advances in microvascular imaging on the examples of murine skeletal muscle and kidney.

### **Imaging of skeletal muscle microvasculature and preclinical therapeutic angiogenesis**

The murine hind limb is a widely used preclinical model to study arteriogenesis and angiogenesis in striate muscle. The current gold standard for quantifying the microvasculature is based on histological cross-sections followed by immunohistochemical visualization of the endothelium. The fact that most capillaries are running in parallel to the muscle fibers make the “capillary-to-fiber ratio” and “capillary density per field of view” simple estimation methods.

However, two-dimensional histological approaches do not provide any information about the 3D vascular angioarchitecture and hierarchical assembly, connectivity, vascular tortuosity, changes in vascular diameter and vascular pattern. Serial sectioning followed by 3D reconstruction is very time-consuming, the alignment is often a huge challenge and in fact is performed very seldom [5, 6]. Vascular corrosion casts technique followed by scanning electron microscopy overcomes these limitations and has been commonly used in the past [7]. The major limitation is the visualization of only the superficial layer and, therefore, reliable quantification. In addition, due to corrosion technique the tissue surrounding the vessels is completely digested, which impairs the detection of the location and mapping of the vessels.

In summary, the entire field of vascular biology has a considerable demand for new and trustworthy high-resolution vascular 3D imaging, which would allow rapid visualizing and quantification of the microvasculature [8].

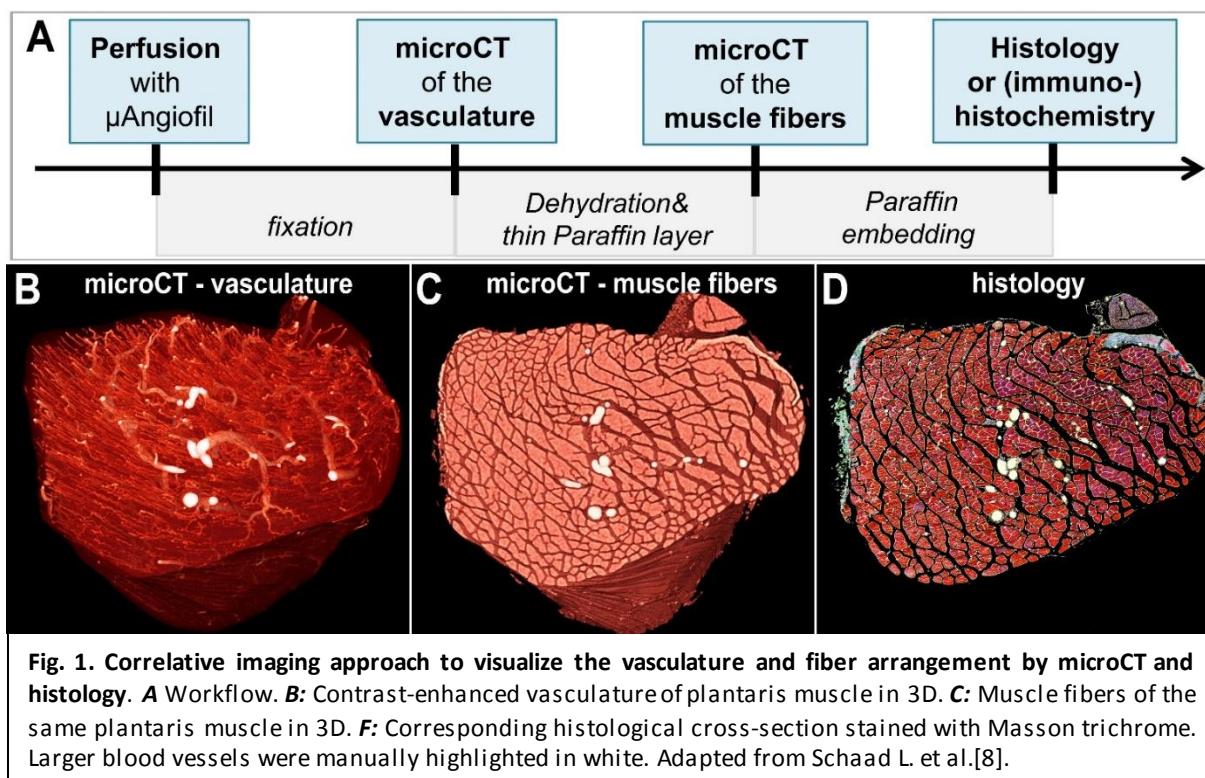
#### **Micro-computed tomography (microCT) and 3D vascular imaging**

Despite of the almost microscopic resolution provided by the current microCT equipment, the vasculature cannot be distinguished from the surrounding soft tissue without a radiopaque contrast agent [9]. Different types of compounds have been used to visualize the vasculature of the heart, liver, kidney, lungs, the hind limb and in murine tumors [10-16]. However, those studies were limited in terms of (i) resolution: usually demonstrating microvessels with diameter between 20 and 50  $\mu\text{m}$ ; (ii) volume of interest: frequently incising the resolution by reducing the area of interest, (iii) filling properties of the compound: often with a relatively high viscosity and thus poor perfusion properties [9, 13].

The combination of vascular corrosion casting followed by microCT visualization has been used for imaging of solitary microvessels in small volumes, for example visualization of individual glomeruli [17]. This technique, however did not overcome the limitation of the vascular casting methodology

(see above). Until recently, visualizing capillaries *in situ* by microCT, without prior tissue maceration, seemed unachievable [8, 17-20].

Recently, a correlative *ex vivo* imaging approach has been introduced, which



allows investigating the murine hind limb vasculature and its surrounding tissue from the whole organ to the capillary level. The established three-step protocol uses microCT (with the polymer-based contrast agent  $\mu$ Angiofil) to non-destructively obtain 3D morphological information of the vasculature and the musculoskeletal system, and the standard (immuno-)histochemistry provides complementary 2D information within the same very sample at the microscopic level (Fig. 1). We call this approach microangiCT ( $\mu$ ACT).

Before focusing on single muscles a microCT scan of the entire murine hind limb can be done providing an excellent overview of its musculoskeletal system (Fig.2). Since the scanning procedure is non-destructive, the sample remains

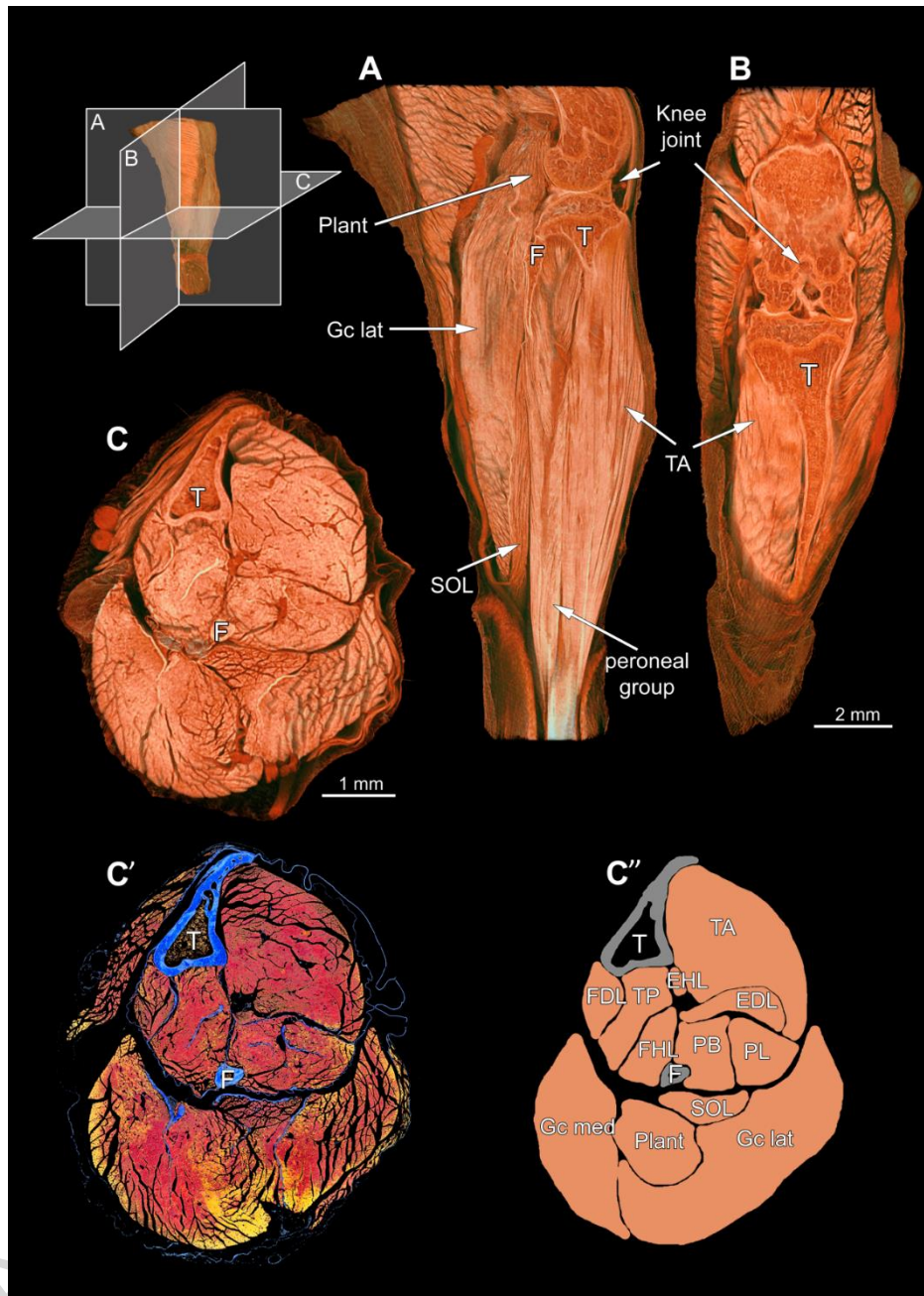


**Fig. 2. Musculoskeletal system of the left murine lower hind limb.** *A* sagittal, *B* coronal and *C* transverse virtual sections through the hind limb as imaged by microCT. Voxel side length: 2.99  $\mu\text{m}$ . *C'* Corresponding histological cross-section stained for Azan Trichrom (blue: bones and connective tissue, red-yellow: muscle tissue). *C''* Scheme with labelled muscles. T= tibia, F = fibula, TA = tibialis anterior, EDL = extensor digitorum longus, EHL = extensor hallucis longus, PB = peroneus brevis, PL = peroneus longus, FDL= flexor digitorum longus, TP = tibialis posterior, FHL = flexor hallucis longus, SOL = soleus, Plant = plantaris, Gc med = gastrocnemius medialis, Gc lat = gastrocnemius lateralis. Adapted from Schaad L. et al.[8].

intact and can be processed for further histology (Fig. 2*C'*) or single muscles can be scanned at even higher detail resolution. The high-resolution  $\mu\text{aCT}$ -scans can provide not only the visualization of the bigger and middle-sized vessels, but the complete microvasculature including the finest capillaries (Fig. 3).

Besides remarkable visualization, the obtained high-quality  $\mu$ CT-data provide an excellent starting point for the quantitative analysis of the vasculature. Due to high and homogenous X-ray absorption of  $\mu$ Angiofil as well as its continuous filling, the  $\mu$ CT-datasets do not need an extensive post-processing for segmenting the vasculature. Robust and relatively swift segmentation of the vasculature is a prerequisite for subsequent quantitative analysis including skeletonization. Once the skeleton is obtained, a more detailed analysis of the vasculature can be performed. Not only the hierarchy of the vascular tree, but also the parameters like connectivity, tortuosity, changes in vascular pattern can be therefore analyzed [8]. The analysis of whole vascular networks and parts thereof, down to “microvascular units”, the smallest functional units for blood flow regulation [21], can be performed and used for future simulations of the mechanisms of the blood flow regulation at different levels.

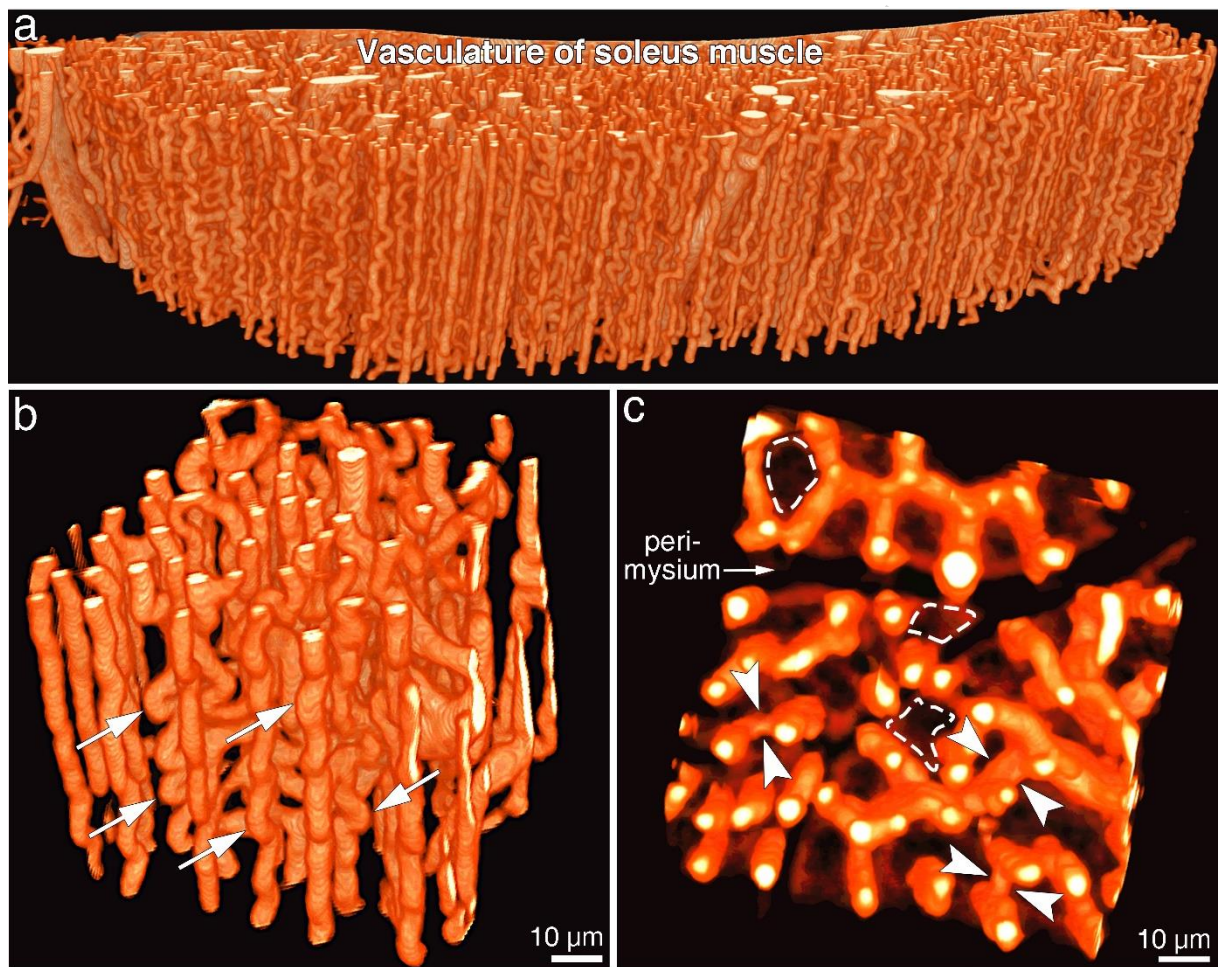


**Fig. 3. Microangiography of the vasculature of the skeletal muscle.** Panel a: overview of the 500µm-thick slice of the murine soleus muscle. Panel b and c represent a subvolume of the volume in a: the capillaries with their connections and tortuosity are clearly and unambiguously visualized (arrows, panel b). In panel c the perimysium as well as borders of the single muscle fiber cells can be easily recognized (*dashed line*).

The overview scan at a lower resolution is very suitable for defining sites of

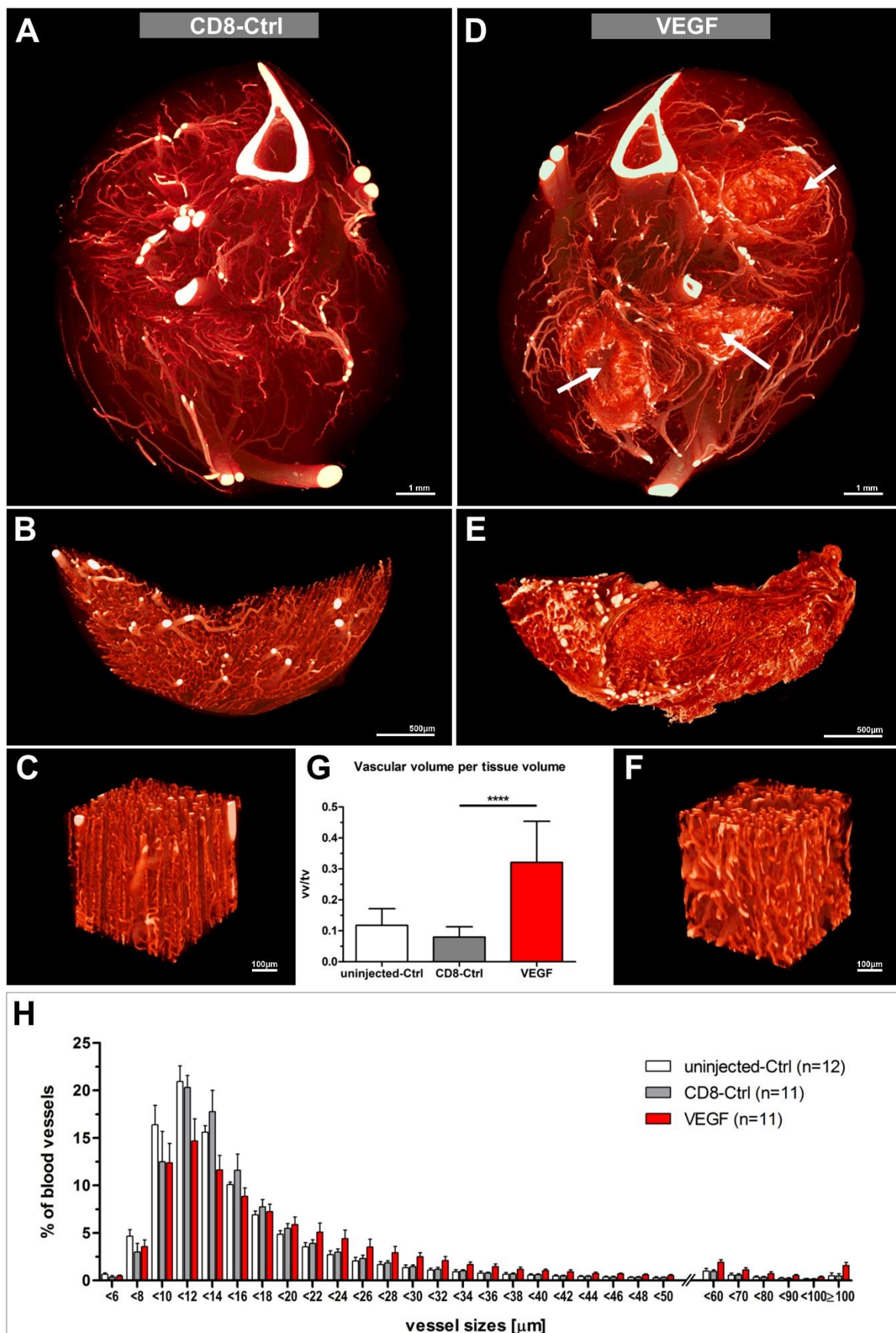


**Fig. 4. Therapeutic application of VEGF-transduced myoblasts.** **A, D** Vascular microCT-scans of CD8-control (A) and VEGF-treated (D) contralateral hind limbs respectively (voxel side length: 2.58 μm). VEGF-injection sites are indicated by arrows. **B-F** High-resolution microCT-scans of the solei muscles (B,E) and regions of interest at higher magnification (C,F) (voxel side length: 0.92 μm). **G** Vascular volume measurements. Vascular volume (vv) per tissue volume (tv) within a given injection or control site. \*\*\*\* p < 0.0001. **H** Vessel size distribution. Histogram presenting the relative proportion of a given vessel size. Vessel diameters are given in μm. Measurements were conducted on 20 equidistant virtual sections per sample. Reproduced from Schaad L. et al.[8].

interest. In a recent study, it was used for revealing the sites of local injection of VEGF-transduced myofibroblasts [8]. Later on, the defined sites of interests within single muscles were rescanned at a higher resolution and subvolumes within the volumes of interest were used for the straightforward quantitative analysis (Fig. 4). Besides unambiguous visualization, the presented  $\mu$ CT-based approach can provide the quantitative differences between the control and treated sites (Fig. 4G, H). Moreover, in the mentioned study the  $\mu$ CT-approach has also been successfully validated using immunohistochemistry within the same samples [8].

Altogether, the *ex vivo*  $\mu$ CT-approach is a reliable and straightforward method for the qualitative and quantitative assessment of the microvasculature of the murine skeletal muscle, which also enables correlative morphology after non-destructive microCT-scans.

### ***Ex vivo* microangioCT in kidney research and kidney morphometry**

Studying of kidney disease in experimental animal models is indispensable for a better understanding of kidney-related pathologies in humans. The main morphological characteristics, which are used for delineating the renal function, are glomerular number ( $N_{\text{glom}}$ ) and glomerular volume. Since decades, these parameters are known to correlate with the renal function: Hayman and coworkers suggested the association of low  $N_{\text{glom}}$  with renal insufficiency and hypertension already in the 1930s [22]. The accurate estimation of these parameters has become increasingly crucial, since they describe the morphological substrate for the renal function and their alterations can provide insights into the pathophysiological processes responsible for development and progression of nephropathies and various “kidney-related” pathologies [23, 24].

The microCT with  $\mu$ Angiofil provides, besides the vascular imaging, also the structural information which can be used for quantitative analysis, including a stereological approach, e.g., for kidney morphometry [25].

The current methodological gold standard in kidney morphometry was introduced in 1992 [26]. It is the physical fractionator/disector method which is often combined with the Cavalieri principle for kidney volume estimation [27, 28]. The important advantage of this approach is its unbiasedness. The main disadvantages are that it is: 1) destructive (the whole kidney has to be sectioned), and 2) extremely time-consuming (at least 4-6 working days per murine or rat kidney) [29]. The mentioned shortcomings render this approach unpopular [27]. Counting of glomeruli after kidney maceration is another established method, which is an even more destructive method [30]. Using this approach, no information on the location of individual glomeruli nor any further structural information on the kidney and its vasculature can be obtained.

Recently, further potentially promising approaches have been introduced, including high-field magnetic resonance imaging with cationized-ferritin labelling or lightsheet microscopy [25, 30, 31]. Unfortunately, those methods also have some critical drawbacks, e.g., the high-field MRI suffers from relatively poor resolution and requires advanced lab equipment. And none of the both mentioned methods provides reliable 3D-visualization of the vasculature of the whole kidney [25]. In that sense, the contrast-enhanced micro-CT is more auspicious. This approach has been constantly refined for renal studies focusing on kidney vasculature and vasculature-related kidney pathologies, e.g., chronic kidney disease or kidney fibrosis [32-34]. In the last decades, the contrast-enhanced microCT-based imaging of the kidney was mainly limited to large and middle-sized vessels due to incomplete perfusion as well as low resolution of the available scanners. Modern microCT-scanners can provide the necessary detail resolution and the available contrast agents (e.g.,  $\mu$ Angiofil) enable complete perfusion with strong and homogenous signal. This

makes the microangiCT with  $\mu$ Angiofil a method of choice for many renal studies [25].

Shortly after perfusion and harvesting of a lab rodent kidney, microCT-datasets

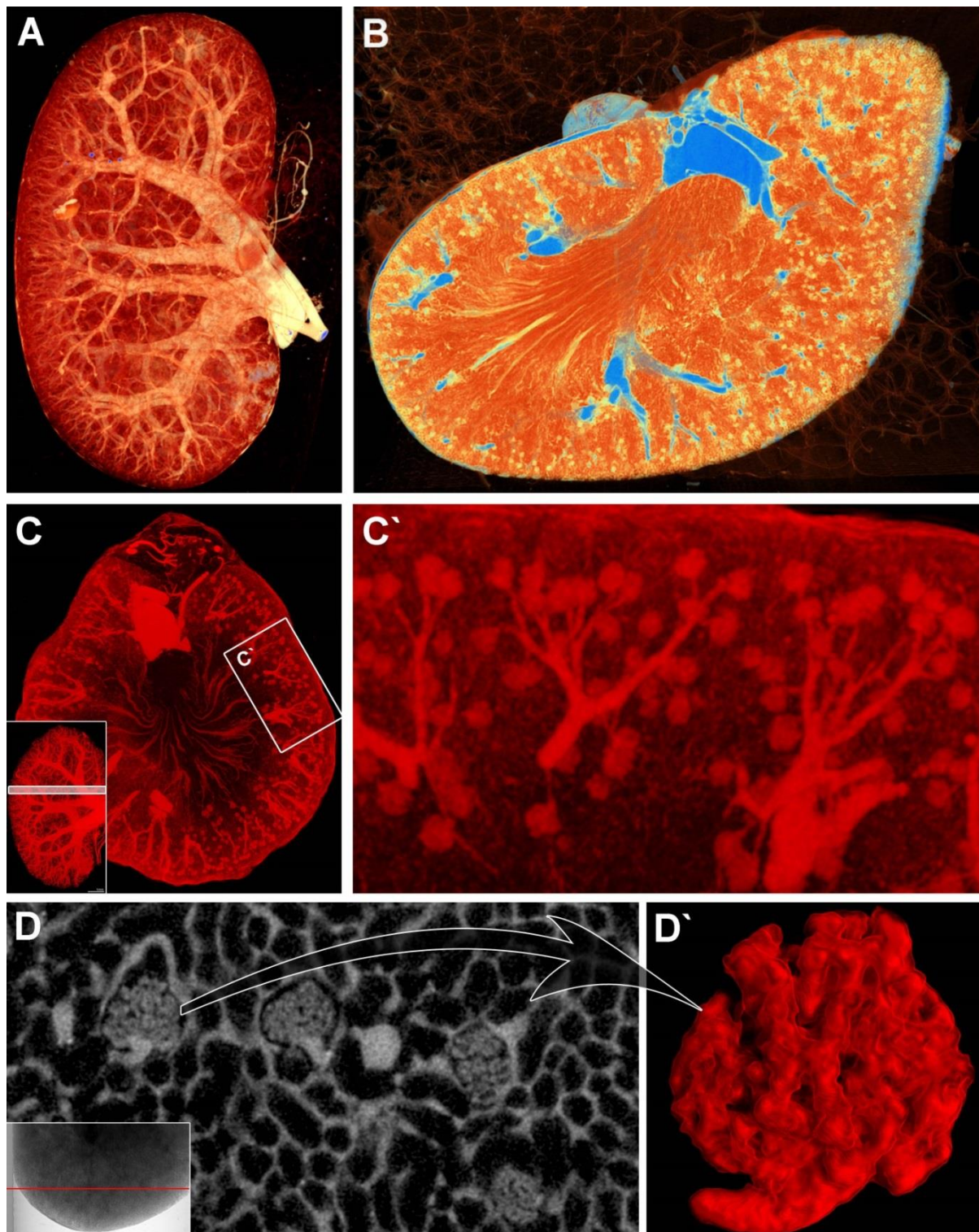


**Fig. 5. Various visualization modalities of the kidney vasculature and glomeruli.** Panel A represents the reconstructed 3D-stack of the  $\mu$ CT-dataset with the focus onto the vasculature of the kidney (bigger vessels are presented in yellow). Panel B represents the virtual section through the dataset using another transfer function: visualization is focused on kidney tissue (bigger vessels are displayed blue, microvessels and glomeruli are seen as yellow structures; tissue is red). Panels C-C' represent the visualization focused onto the glomeruli: panel C displays a volume rendering of a virtual 500 $\mu$ m-thick slice as indicated with the white box in the insert in the lower left corner of the image. The white frame in C indicates the site with the glomeruli shown at higher magnification in panel C'. Panel D-D' represents the advanced visualization option:  $\mu$ CT at a higher resolution (voxel side size =0.59 $\mu$ m). The insert in the panel D indicates the virtual section level displayed in D. The 3D-volume rendering of the microvasculature of glomerulus marked in D is displayed in D'. Reproduced from Hlushchuk R. et al.[4].

are recorded and can be used for the visualization of the various aspects, e.g.: 1) kidney as whole and its (macro)vasculature (Fig. 5A); 2) kidney tissue with highlighted vascular structures as seen on virtual sections through the dataset (Fig. 5B); 3) distribution of the glomeruli at low and high magnifications (Fig. 5C-C`), etc. In that way, the obtained datasets enable screening for potential sites of interest for further exploration by rescanning at a higher resolution (Fig. 5D-D`) or/and subsequent histological investigation (Fig. 6). The intravascular solidified  $\mu$ Angiofil does not interfere with processing for histology. Furthermore, its inherent fluorescence simplifies the search for the corresponding site of interest within the  $\mu$ CT-dataset (Fig. 6). It is a great advantage for subsequent correlative microscopy. Another remarkable possibility is to use the obtained datasets for a quantitative analysis using the stereological approach. The stereological analysis on  $\mu$ CT-based images can be started within hours, instead of multiple days when using a classical histology-based approach. Besides saving a lot of time and labor, such a  $\mu$ CT-based quantitative analysis does not destruct the sample, provides reliable data and is virtually artefact-free (see [25] for more details).

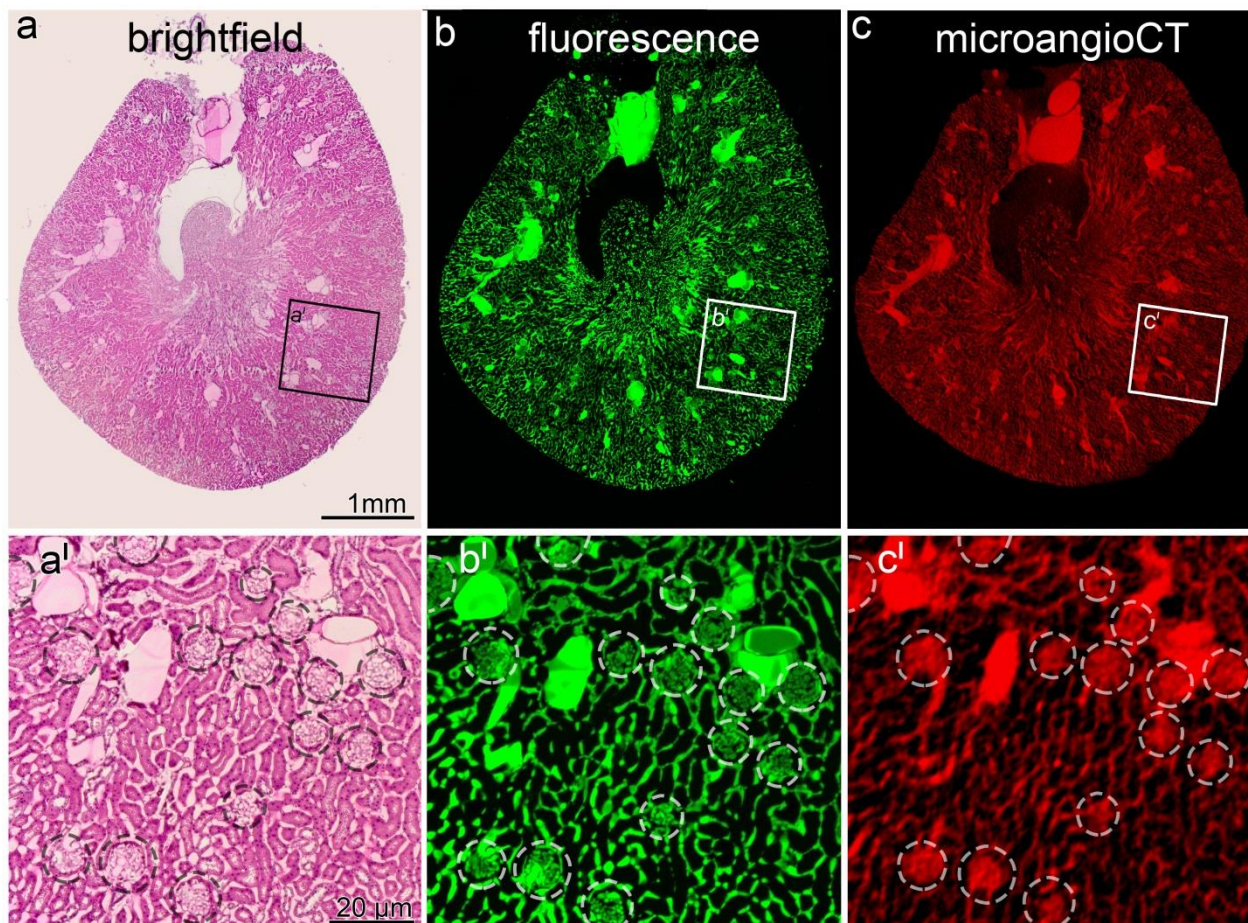


**Fig. 6. Correlative microscopy: visualization of corresponding sites using  $\mu$ CT-data and histological approach.** After image acquisition, the fixed kidney was processed for histological sectioning and investigation. Panels a - b - c display the visualization of the same level (section) of the same kidney using brightfield (a & a') and fluorescence (b & b') microscopy as well as  $\mu$ CT (c & c'). The green signal in b and b' comes from autofluorescent  $\mu$ Angiofil<sup>®</sup> that is polymerized within the vessels. This feature makes the registration between histology and  $\mu$ CT an easy task due to orientation onto the bigger vessels. The panels a''-c'' display at higher magnification the regions indicated in a-c. The glomeruli are indicated with circles in a''-c''. Reproduced from Hlushchuk R. et al.[4].

## Conclusions

There are many methods to visualize the vasculature in 2D. The number of methods that are able to do it in 3D is considerably smaller, with most of them having major drawbacks like low spatial resolution (incl. anisotropic or axial resolution for lightsheet microscopy), limited penetration into the depth of the sample (in case of laser confocal or multi-photon microscopy). The current gold standard approaches for detailed 3D visualization of blood vessels include serial sectioning or vascular corrosion casting. These methods are destructive, time-consuming and entail various difficulties, as mentioned above. On the contrary, microangiography allows time-efficient and non-destructive 3D imaging [8].

Upon scanning, the chemically fixed sample is still available for further analysis. This circumstance enables combining microCT with subsequent histology or electron microscopy, i.e., correlative morphology. The solidified  $\mu$ Angiofil stays intravascular and autofluoresces, making the registration of the histological sections within the microCT-dataset an easy task (Fig. 6) [25].

The approach provides detailed 3D information enabling 3D-skeletonization of the organ vasculature and its further analysis with the help of already publicly available tools [25, 32, 35]. In the field of kidney research, this is a crucial advantage over the recently introduced approaches of kidney analysis using high-field MRI or lightsheet microscopy with *in vivo* antiCD31-labelling [25, 30].

Another plus of the contrast-enhanced microCT with  $\mu$ Angiofil is the blue color of the  $\mu$ Angiofil, which enables direct visual control of the perfusion success. Due to its low viscosity during perfusion, even the finest capillaries can be filled continuously. Moreover, its solidification brings extra stability to the sample during rather long microCT-scanning sessions. Nevertheless, it does not interfere with the eventual post-processing for histology. Furthermore, samples were stored in fixative over several months with the contrast agent retaining stability. Hence, as long as the samples are not physically destroyed through, e.g., sectioning, they can be rescanned any time [8]. The analogue situation is true for the microCT-datasets: they are stored and can be reanalyzed at any time. Another advantageous feature of  $\mu$ Angiofil is its inherent fluorescence, which renders tedious capillary staining for fluorescence microscopy superfluous (Fig. 6) [8].

Probably the only significant limitation of the described approach is that it can be used only *ex vivo* (=no longitudinal studies).

In spite of this drawback, microangioCT with  $\mu$ Angiofil is a relatively simple and straightforward tool with a broad application range for studying physiological and pathological alterations in the microvasculature of any organ. It provides microvascular imaging at unprecedented level and enables correlative

microscopy. The aforementioned features as well as high reproducibility make it a reliable partner in a very broad spectrum of research studies where microvasculature is of significant importance. In particular, it is a gainful approach for preclinical studies dealing with novel therapeutic treatment strategies or drug candidates, in which the pro- and antiangiogenic must be reliably evaluated, qualitatively as well as quantitatively.

1. Carmeliet, P. and R.K. Jain, *Molecular mechanisms and clinical applications of angiogenesis*. Nature, 2011. **473**(7347): p. 298-307.
2. Kraljevic, S., P.J. Stambrook, and K. Pavelic, *Accelerating drug discovery*. EMBO Rep, 2004. **5**(9): p. 837-42.
3. Singh, M. and N. Ferrara, *Modeling and predicting clinical efficacy for drugs targeting the tumor milieu*. Nat Biotechnol, 2012. **30**(7): p. 648-57.
4. Hlushchuk, R., et al., *Zebrafish Caudal Fin Angiogenesis Assay-Advanced Quantitative Assessment Including 3-Way Correlative Microscopy*. PLoS One, 2016. **11**(3): p. e0149281.
5. Bussolati, G., C. Marchio, and M. Volante, *Tissue arrays as fiducial markers for section alignment in 3-D reconstruction technology*. J Cell Mol Med, 2005. **9**(2): p. 438-45.
6. Barre, S.F., et al., *Efficient estimation of the total number of acini in adult rat lung*. Physiol Rep, 2014. **2**(7).
7. Djonov, V. and P.H. Burri, *Corrosion Cast Analysis of Blood Vessels*, in *Methods in Endothelial Cell Biology*, H.G. Augustin, Editor. 2004, Springer Berlin Heidelberg: Berlin, Heidelberg. p. 357-369.
8. Schaad, L., et al., *Correlative Imaging of the Murine Hind Limb Vasculature and Muscle Tissue by MicroCT and Light Microscopy*. Sci Rep, 2017. **7**: p. 41842.
9. Perrien, D.S., et al., *Novel methods for microCT-based analyses of vasculature in the renal cortex reveal a loss of perfusable arterioles and glomeruli in eNOS<sup>-/-</sup> mice*. BMC Nephrol, 2016. **17**: p. 24.
10. Ward, N.L., et al., *Angiopoietin-1 Causes Reversible Degradation of the Portal Microcirculation in Mice*. The American Journal of Pathology, 2004. **165**(3): p. 889-899.
11. Sangaralingham, S.J., et al., *Cardiac Micro-Computed Tomography Imaging of the Aging Coronary Vasculature*. Circulation: Cardiovascular Imaging, 2012. **5**(4): p. 518-524.
12. Ghanavati, S., et al., *A perfusion procedure for imaging of the mouse cerebral vasculature by X-ray micro-CT*. Journal of Neuroscience Methods, 2014. **221**: p. 70-77.
13. Vasquez, S.X., et al., *Optimization of microCT imaging and blood vessel diameter quantitation of preclinical specimen vasculature with radiopaque polymer injection medium*. PLoS One, 2011. **6**(4): p. e19099.
14. Savai, R., et al., *Evaluation of Angiogenesis Using Micro-Computed Tomography in a Xenograft Mouse Model of Lung Cancer*. Neoplasia, 2009. **11**(1): p. 48-56.
15. Cristofaro, B., et al., *Dll4-Notch signaling determines the formation of native arterial collateral networks and arterial function in mouse ischemia models*. Development, 2013. **140**(8): p. 1720-9.
16. Ehling, J., et al., *Micro-CT Imaging of Tumor Angiogenesis*. The American Journal of Pathology, 2014. **184**(2): p. 431-441.
17. De Spiegelaere, W., et al., *Expression and localization of angiogenic growth factors in developing porcine mesonephric glomeruli*. J Histochem Cytochem, 2010. **58**(12): p. 1045-56.
18. Debbaut, C., et al., *Analyzing the human liver vascular architecture by combining vascular corrosion casting and micro-CT scanning: a feasibility study*. J Anat, 2014. **224**(4): p. 509-17.
19. Nebuloni, L., et al., *A Novel In Vivo Vascular Imaging Approach for Hierarchical Quantification of Vasculature Using Contrast Enhanced Micro-Computed Tomography*. PLoS One, 2014. **9**(1): p. e86562.

20. Krucker, T., A. Lang, and E.P. Meyer, *New polyurethane-based material for vascular corrosion casting with improved physical and imaging characteristics*. *Microsc Res Tech*, 2006. **69**(2): p. 138-47.
21. Bagher, P. and S.S. Segal, *Regulation of blood flow in the microcirculation: role of conducted vasodilation*. *Acta Physiol (Oxf)*, 2011. **202**(3): p. 271-84.
22. Hayman, J.M., et al., *Experimental Hyposthenuria*. *J Clin Invest*, 1939. **18**(2): p. 195-212.
23. Hoy, W.E., et al., *Nephron number, glomerular volume, renal disease and hypertension*. *Curr Opin Nephrol Hypertens*, 2008. **17**(3): p. 258-65.
24. Samuel, T., et al., *Applicability of the glomerular size distribution coefficient in assessing human glomerular volume: the Weibel and Gomez method revisited*. *J Anat*, 2007. **210**(5): p. 578-82.
25. Hlushchuk, R., et al., *Cutting-edge microangio-CT: new dimensions in vascular imaging and kidney morphometry*. *Am J Physiol Renal Physiol*, 2018. **314**(3): p. F493-F499.
26. Bertram, J.F., et al., *Total numbers of glomeruli and individual glomerular cell types in the normal rat kidney*. *Cell Tissue Res*, 1992. **270**(1): p. 37-45.
27. Bertram, J.F., et al., *Why and how we determine nephron number*. *Pediatr Nephrol*, 2014. **29**(4): p. 575-80.
28. Nyengaard, J.R., *Stereologic methods and their application in kidney research*. *J Am Soc Nephrol*, 1999. **10**(5): p. 1100-23.
29. Heilmann, M., et al., *Quantification of glomerular number and size distribution in normal rat kidneys using magnetic resonance imaging*. *Nephrol Dial Transplant*, 2012. **27**(1): p. 100-7.
30. Klingberg, A., et al., *Fully Automated Evaluation of Total Glomerular Number and Capillary Tuft Size in Nephritic Kidneys Using Lightsheet Microscopy*. *J Am Soc Nephrol*, 2017. **28**(2): p. 452-459.
31. Chacon-Caldera, J., et al., *Fast glomerular quantification of whole ex vivo mouse kidneys using Magnetic Resonance Imaging at 9.4 Tesla*. *Z Med Phys*, 2016. **26**(1): p. 54-62.
32. Ehling, J., et al., *Quantitative Micro-Computed Tomography Imaging of Vascular Dysfunction in Progressive Kidney Diseases*. *J Am Soc Nephrol*, 2016. **27**(2): p. 520-32.
33. Heinzer, S., et al., *Hierarchical microimaging for multiscale analysis of large vascular networks*. *Neuroimage*, 2006. **32**(2): p. 626-36.
34. Xu, R., et al., *Polycystic kidneys have decreased vascular density: a micro-CT study*. *Microcirculation*, 2013. **20**(2): p. 183-9.
35. Nordsletten, D.A., et al., *Structural morphology of renal vasculature*. *Am J Physiol Heart Circ Physiol*, 2006. **291**(1): p. H296-309.